



# Investigating broad absorption line quasars with SDSS and UKIDSS

Natasha Maddox<sup>1</sup> and P. C. Hewett<sup>2</sup>

<sup>1</sup> Astrophysikalisches Institut Potsdam, An der Sternwarte 16, 14482 Potsdam, Germany  
e-mail: nmaddox@aip.de

<sup>2</sup> Institute of Astronomy, University of Cambridge, Madingley Road, Cambridge CB3 0HA, UK

## Abstract.

The SDSS contains the largest set of spectroscopically confirmed broad line quasars ever compiled. Upon its completion, the UKIDSS LAS will provide a near-infrared counterpart to the SDSS, reaching 3 magnitudes deeper than 2MASS over a 4000 square degree area within the SDSS footprint. Combining the SDSS optical and UKIDSS near-infrared data, allows a new insight into the photometric and spectroscopic properties of broad absorption line quasars (BALQSOs) relative to the quasar population as a whole.

An accurate estimate of the intrinsic BALQSO fraction is essential for determining the BAL cloud covering fraction and the implications for the co-evolution of accreting supermassive black holes and their host galaxies. Defining a  $K$ -band limited sample of quasars makes clear the significantly redder distribution of  $i - K$  colours of the BALQSOs. The BALQSO  $i - K$  colour distribution enables us to estimate a lower limit to the intrinsic BALQSO fraction, computed to be  $\sim 30$  percent, significantly larger than the optical fraction of 15–20 percent found by several authors. We combined the high-quality SDSS spectra of the quasar sample to make several composite spectra based on  $i - K$  colour, and the properties of these composites are compared to a composite spectrum of unreddened quasars. If the origin of the wavelength dependent differences between the red and unreddened objects is ascribed to attenuation by dust, we find that the extinction curve of the material is intermediate in form between the steep SMC-like extinction curve and the recent, empirically determined, extinction curve presented by Gaskell & Benker (2007).

**Key words.** Quasars: general – surveys – infrared: general

## 1. Introduction

The fraction of quasars exhibiting broad absorption lines (BALs) in their spectra blueward of high ionisation lines, primarily CIV, is poorly constrained, with several authors arriving at seemingly discrepant results. A complete

census of the BAL quasar (BALQSO) population will help constrain both the absorber geometry and covering fraction.

There are indications that BALQSOs have somewhat redder continua than nonBALQSOs (see Reichard et al. 2003, for example). If the reddening is due to dust associated with the quasars, then the number of BALQSOs present

in optically selected samples is an underestimate of the total population. Observations at longer wavelengths less affected by dust extinction, such as the near-infrared (NIR), alleviate this issue. This study aims to exploit the overlap between the SDSS and the newly available large area, deep NIR data provided by the UKIRT Infrared Deep Sky Survey (UKIDSS, Lawrence et al. 2007) to investigate the NIR properties of BALQSOs, the optical–NIR colours of BALQSOs with respect to the nonBALQSO population, and constrain the shape of the extinction curve causing the reddening.

## 2. Data

The optical photometry and spectra are taken from the SDSS DR5 quasar catalogue (Schneider et al. 2007). These 77 429 quasars are then matched to data contained within the UKIDSS Large Area Survey Data Release 3 (LAS DR3+), limited to  $K \leq 17.0$ . Only quasars within the redshift range  $1.70 \leq z \leq 4.38$  are retained to ensure spectral coverage of the CIV 1549Å emission line and the blueward continuum, resulting in a final sample of 2051 objects. This redshift range coincides with that used in the SDSS DR3 BALQSO study of Trump et al. (2006). Note that all magnitudes quoted in this work are based on the Vega system, with the SDSS AB-magnitudes converted to the Vega system using the offsets in Hewett et al. (2006).

As one aim of this study is to determine whether BALQSOs are redder than the non-BALQSO population, the reddest objects must be included. Figure 1 illustrates the  $i-K$  values accessible at a series of  $K$ -band magnitude limits for the SDSS Main Survey area (top) and the Stripe 82 area only (bottom). Comparing the top and bottom panels shows that the deeper Stripe 82 data, which isn't subject to the  $i \leq 18.7$  magnitude limit of the SDSS quasar selection algorithm, reaches larger  $i-K$  values for a given  $K$ -band magnitude. Therefore, for statistical purposes, the sample is divided into three subsamples. Stripe 82 data is used for  $K \leq 17.0$  and  $K \leq 16.0$  subsamples, and the SDSS Main Survey area is used for  $K \leq 15.0$  statistics. The

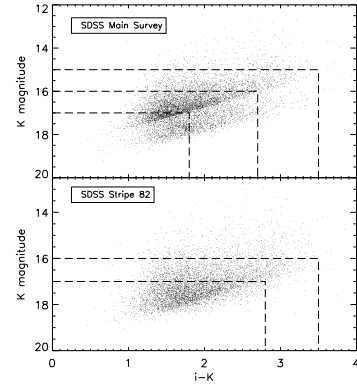


**Fig. 1.** Colour-magnitude diagrams for matched SDSS–UKIDSS quasars, showing only data from the SDSS Main Survey area (top) and from the SDSS Stripe 82 area (bottom). The density ridge seen in the top panel is due to the  $i \leq 18.7$  magnitude restriction in the quasar selection algorithm.

$K \leq 17.0$  subsample from the Stripe 82 data is found to suffer from incompleteness due to the limited  $i-K$  range, but is included for illustration.

### 2.1. Balnicity index

In order to compute the balnicity index (BI, Weymann et al. 1991), a ‘continuum fit’ is required. A high SNR composite quasar spectrum was constructed from a large number of nonBALQSOs. Each quasar spectrum is divided by the redshifted composite, and a power-law fit ( $f(\lambda) \propto \lambda^a$ ) is used to characterise the difference in slope between the quasar and composite spectra. The overall shape of the composite spectrum is adjusted using the power-law fit. Then, an iterative procedure further modifies the shape of the composite on smaller scales using the systematic differences between the composite and the quasar spectrum. Pixels in the quasar spectra that fall below the adjusted composite by more than a specified threshold (i.e. broad absorption lines) are excluded from the fitting process. The BI is then computed for each continuum-normalised spectrum, using the formula described in Appendix A of Weymann et

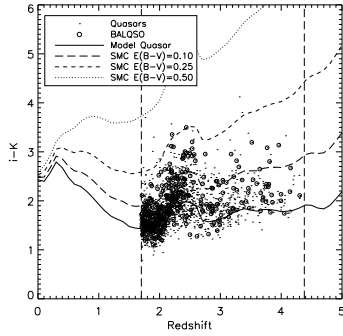


**Fig. 2.** The  $i - K$  vs redshift colours of the full sample of 2051  $1.70 \leq z \leq 4.38$ ,  $K \leq 17.0$  quasars, with BALQSOs shown as open circles.

al. (1991). Any object with  $BI > 2$  is classified as a BALQSO.

### 3. Optical–NIR colour

Figure 2 shows the  $i - K$  colours as a function of redshift for the full sample of 2051  $K \leq 17.0$  quasars, with BALQSOs shown as open circles. A K-S test on the  $K \leq 16.0$  sample indicates that the  $i - K$  colours of BALQSOs are redder than the colours of the nonBALQSO population with high significance, with the  $i - K$  distribution for the BALQSOs having a more extended red tail. Overplotted are quasar tracks derived from a model quasar as described in Maddox et al. (2008). The solid line shows the  $i - K$  colour for an unreddened quasar, with the long dashed, short dashed and dotted lines indicating the colours for the model quasar subjected to increasing amounts of SMC-like dust reddening. If the reddening of the BALQSOs is due to dust, the position of an object on the  $i - K$  vs redshift plane provides an estimate of the amount of extinction it is suffering.

### 4. BALQSO fraction

Estimates of the fraction of BALQSOs with respect to the entire quasar population range from  $\sim 10$  percent (Trump et al. 2006) to corrected fractions of  $> 20$  percent (Hewett & Foltz 2003, Knigge et al. 2008). Recent work by Dai et al. (2008), using the SDSS DR3

BALQSO list compiled by Trump et al. (2006) in conjunction with NIR data from 2MASS (Skrutskie et al. 2006) shows that the BALQSO fraction increases as the quasar sample is selected at longer wavelengths.

The computed uncorrected BALQSO fractions for the various subsamples are compiled in Table 1. The  $K \leq 17.0$  BALQSO fractions are underestimates, due to their restricted range in  $i - K$  colour. The  $K \leq 16.0$  fraction in the Stripe 82 reaches large  $i - K$  values and relatively faint  $K$ -band magnitude, and thus provides the best estimate of the BALQSO fraction. The value of 27 percent is significantly larger than the  $\sim 10$  percent found using the SDSS DR3 sample, and is in good agreement with results from Maddox et al. (2008), who find a BALQSO fraction of  $\sim 25$  percent from a sample of quasars selected based on their  $K$ -band excess. As these samples are flux-limited in the  $K$ -band, the corrections due to dust obscuration are small, in contrast with the large corrections that are needed at optical wavelengths.

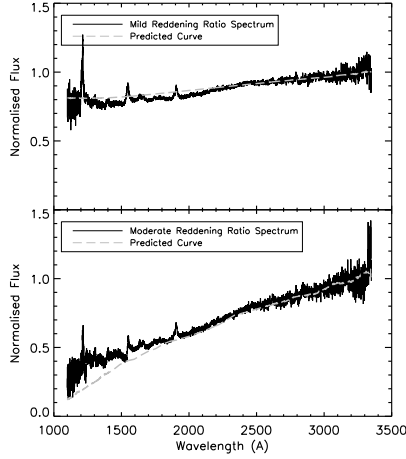
### 5. Composite spectra

Assuming an object’s position on the  $i - K$  vs redshift plot (Figure 2) is entirely due to dust reddening,  $E(B - V)$  values for each quasar can be computed. Quasars with  $E(B - V) < 0.05$  are designated as unreddened, objects with  $0.05 < E(B - V) < 0.10$  mildly reddened, and those with  $E(B - V) > 0.1$  moderately reddened. Composite spectra are created for each of the three categories. Both BALQSOs and nonBALQSOs are included in the composites. The results do not change if only BALQSOs are included, only the signal-to-noise ratio of the composites is lower due to fewer contributing spectra.

Dividing the reddened composite spectra by the unreddened composite effectively produces extinction curves. The top panel of Figure 3 shows the mildly reddened composite ratio spectrum, overplotted with a dust reddening curve assuming dust of the form from Gaskell & Benker (2007) with an  $E(B - V)$  value representative of the objects used to create the composite. As seen, the Gaskell

**Table 1.** BALQSO fractions from SDSS and the KX sample from Maddox et al. (2008)

Survey Area	SDSS Stripe 82		SDSS Main	KX
Magnitude Limit	$K \leq 17$	$K \leq 16$	$K \leq 15$	$K \leq 16$
BALQSO Fraction	17%	27%	18%	25%

**Fig. 3.** (Top) Composite ratio spectrum for mildly reddened quasars, overplotted with a Gaskell & Benker extinction curve. (Bottom) Composite ratio spectrum for moderately reddened quasars, overplotted with an SMC extinction curve.

& Benker curve is not red enough at short ( $\lambda < 2200 \text{ \AA}$ ) wavelengths. The discrepancy increases with the moderately reddened composite. The bottom panel shows the moderately reddened composite ratio spectrum overplotted with an SMC-type dust extinction curve. The SMC curve is too red at short wavelengths.

## 6. Conclusions

Combining data from SDSS and UKIDSS it is apparent that BALQSOs have redder optical–NIR colours than the nonBALQSO population. The fraction of the quasar population exhibiting the BAL phenomenon in samples selected in the  $K$ -band is found to be as high as 27 percent, much larger than the 10 percent found in optically selected samples. Dividing composite spectra created from quasars with red  $i - K$

colours by an unreddened composite indicates that the reddening is not consistent with either SMC-type dust or dust as postulated by Gaskell & Benker (2007). The extinction curve appears similar to that of the SMC at  $\lambda > 2000 \text{ \AA}$ , but is much less steep at shorter wavelengths, possibly indicating a reduced fraction of very small dust grains. There is also no evidence for a  $2175 \text{ \AA}$  feature as found in Galactic or LMC curves. Our results contrast with several studies based on SDSS quasars (Richards et al. 2003, Hopkins et al. 2004) that find the reddest quasars to have spectral shapes consistent with SMC-type dust. However, these studies focus on lower redshift quasars, and are therefore less sensitive to the departure from SMC dust behaviour seen at  $\lambda < 2000 \text{ \AA}$  in Figure 3.

## References

- Dai, X., Shankar, F., & Sivakoff, G. R. 2008, *ApJ*, 672, 108
- Gaskell, C. M., & Benker, A. J. 2007, *ArXiv e-prints*, 711, arXiv:0711.1013
- Hewett, P. C., Warren, S. J., Leggett, S. K., & Hodgkin, S. T. 2006, *MNRAS*, 367, 454
- Hewett, P. C., & Foltz, C. B. 2003, *AJ*, 125, 1784
- Hopkins, P. F., et al. 2004, *AJ*, 128, 1112
- Knigge, C., Scaringi, S., Goad, M. R., & Cottis, C. E. 2008, *MNRAS*, 386, 1426
- Lawrence, A., et al. 2007, *MNRAS*, 379, 1599
- Maddox, N., Hewett, P. C., Warren, S. J., & Croom, S. M. 2008, *MNRAS*, 386, 1605
- Reichard, T. A., et al. 2003, *AJ*, 126, 2594
- Richards, G. T., et al. 2003, *AJ*, 126, 1131
- Schneider, D. P., et al. 2007, *AJ*, 134, 102
- Skrutskie, M. F., et al. 2006, *AJ*, 131, 1163
- Trump, J. R., et al. 2006, *ApJS*, 165, 1
- Weymann, R. J., Morris, S. L., Foltz, C. B., & Hewett, P. C. 1991, *ApJ*, 373, 23